Measuring pulse-front tilt in ultrashort pulses using GRENOUILLE

Selcuk Akturk, Mark Kimmel, Patrick O'Shea, Rick Trebino

School of Physics, Georgia Institute of Technology, Atlanta, GA 30332-0430, USA
akturk@socrates.physics.gatech.edu

http://www.physics.gatech.edu/frog

Abstract: We show that the spatio-temporal distortion, pulse-front tilt, is naturally, easily, and sensitively measured by the recently demonstrated, extremely simple variation of single-shot second-harmonic generation frequency-resolved optical gating (SHG FROG): GRENOUILLE. While GRENOUILLE traces are ordinarily centered on the zero of delay, a pulse with pulse-front tilt yields a trace whose center is shifted to a nonzero delay that is proportional to the pulse-front tilt. As a result, the trace-center shift reveals both the magnitude and sign of the pulse-front tilt—independent of the temporal pulse intensity and phase. The effects of pulse-front tilt can then easily be removed from the trace and the intensity and phase vs. time also retrieved, yielding a full description of the pulse in space and time.

OCIS codes: (320.7080) Ultrafast devices, (320.7100) Ultrafast measurements

References and links

1. S. Akturk, M. Kimmel, P. O'Shea, and R. Trebino, "Measuring spatial chirp in ultrashort pulses using single-shot Frequency-Resolved Optical Gating," Opt. Express **11**, 68-78 (2003), http://www.opticsexpress.org/abstract.cfm?URI=OPEX-11-1-68
2. Z. Bor, B. Zacz, G. Szabo, M. Hilbert, H.A. Hazim, "Femtosecond pulse front tilt caused by angular dipersion," Opt. Eng. **32**, 2501-2504 (1993).
3. O.E. Martinez, "Pulse Distortions in tilted pulse schemes for ultrashort pulses," Opt. Commun. **59** 229-232, (1986).
4. K. Varju, A.P. Kovacs, G. Kurdi, K. Osvay, "High precision measurement of angular dispersion in a CPA laser," Appl. Phys. B **74** [Suppl.], S259-S263, (2002).
5. B. S. Prade, J. M. Schins, E. T. J. Nibbering, M. A. Franco and A. Mysyrowicz, "A simple method for the determination of the intensity and phase of ultrashort optical pulses" Opt. Commun. **113**, 79-84 (1994).
6. C. Iaconis, C., I.A. Walmsley , "Self-referencing spectral interferometry for measuring ultrashort optical pulses", JQE **35**, 501-509 (1999).
7. C. Dorrer, E.M. Kosik, I.A. Walmsley, "Spatio-temporal characterization of the electric field of ultrashort optical pulses using two-dimensional shearing interferometry", Appl. Phys. B **74** [Suppl.], S209-S217 (2002)
8. Z. Sacks, G. Mourou, R. Danielius, "Adjusting pulse-front tilt and pulse duration by use of a single-shot autocorrelator," Opt. Lett. **26**, 462-464, (2001).
9. D.J. Kane, R. Trebino, "Characterization of arbitrary femtosecond pulses using Frequency-Resolved Optical Gating," IEEE JQE **29**, 571-579, (1993).
10. P. O'Shea, M. Kimmel, X. Gu, and R. Trebino, "Highly simplified ultrashort pulse measurement," Opt. Lett. **26**, 932-934 (2001).
11. R. Trebino, *Frequency-Resolved Optical Gating: The Measurement of Ultrashort Laser Pulses* (Kluwer Academic Publishers, 2002).
12. O.E. Martinez, "Grating and prism compressors in the case of finite beam size," Opt. Soc. Am. B **3**, 929-934, (1986).
13. K. Varju, A.P. Kovacs, K. Osvay, G. Kurdi, "Angular dispersion of femtosecond pulses in a Gaussian beam," Opt. Lett. **27**, 2034-2036, (2002).
14. A. G. Kostenbauder, "Ray-Pulse Matrices: A Rational Treatment for Dispersive Optical Systems," IEEE JQE **26**, 1148-1157 (1990).
15. O.E. Martinez, "Matrix formalism for pulse compressors," IEEE JQE **24**, 2530-2536).

#2097 - $15.00 US Received February 03, 2003; Revised March 01, 2003

1. Introduction

Because their generation involves considerable spatio-temporal manipulations, ultrashort laser pulses commonly suffer from spatio-temporal distortions. The most common such distortions encountered in ultrafast laser laboratories are *spatial chirp* and *pulse-front tilt*. Spatial chirp is the tendency of pulses to have the redder colors on one side of the beam and the bluer colors on the other, and it results from prism pairs and tilted windows. Pulse-front tilt involves the pulse group fronts (intensity contours) tilting with respect to the perpendicular to the propagation direction.

We have recently shown that single-shot second-harmonic-generation frequency-resolved optical gating (SHG FROG) and its experimentally very simple version, GRENOUILLE, easily measure the pulse spatial chirp [1], which is revealed as a shear (tilt) in the otherwise symmetrical measured FROG trace. As with spatial chirp, the main source of pulse-front tilt is devices such as pulse compressors or stretchers, which are standard in essentially all ultrafast lasers and apparatuses. Propagation through a dispersive device causes different frequency components of the beam to propagate at different angles, that is, *angular dispersion*, which also causes pulse-front tilt (see Fig. 1). Indeed, it has been shown that angular dispersion is fundamentally the same phenomenon as pulse-front tilt [2] [The electric field of a pulse with pulse-front tilt can be expressed in the (x,t) domain as $E(x,t-\zeta x)$, which, Fourier transforms from the (x,t) domains to the (k,ω) domains to $E(k-\gamma\omega,\omega)$, that is, a field with angular dispersion.] Thus pulse-front tilt is invariably accompanied by angular dispersion (so a diagnostic for one is also a diagnostic for the other). Therefore, devices like pulse compressors, which, if not aligned correctly, introduce angular dispersion, also introduce significant pulse-front tilt. In principle, a second prism with its inner surface perfectly parallel to that of the first prism completely removes the angular dispersion and pulse-front tilt introduced by the first. However, even minor non-parallelism or beam divergence leaves residual angular dispersion and pulse-front tilt. Devices like pulse compressors use four identical prisms and often yield pulse-front tilt at the output unless aligned perfectly. In two-prism configurations, which use only two prisms and a mirror or mirrors to reflect the beam back on itself, the beam may be diverging or converging while inside the device, causing slight shifts in angle of incidence, and hence pulse-front tilt. There are other possible sources of pulse-front tilt, like slightly wedged optical components. As a result, beams used in ultrafast laser laboratories are frequently contaminated with pulse-front tilt (and angular dispersion).

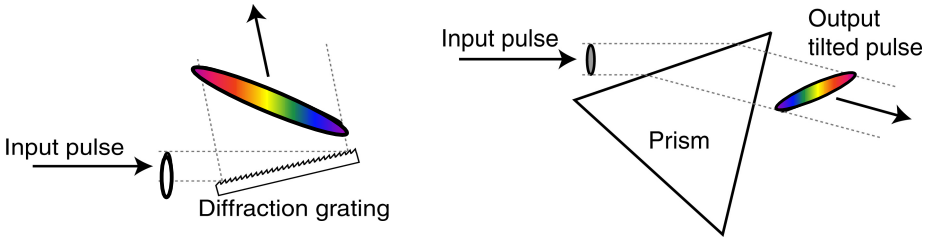

Fig. 1. Elements that introduce angular dispersion also introduce pulse-front tilt.

Indeed, since ultrashort pulses can be very broadband, pulse-front tilt can be significant and problematic. Probably the most significant problem is that pulses with pulse-front tilt are temporally broader than pulses without pulse-front tilt, and the assumption that temporal and spatial evolutions are independent ceases to be valid. Other problems arising due to pulse-front tilt include pulse frequency shifts and spatial profile variations [3].

Despite its ubiquity and potential for mischief in ultrafast experiments, pulse-front tilt is not commonly measured, and only a few diagnostics have been proposed for it. The best existing method, "Spectrally resolved interference (SRI)" [4], is an interferometric method utilizing the spatial fringes formed when two beams cross at an angle. This method provides

#2097 - $15.00 US Received February 03, 2003; Revised March 01, 2003

high precision measurement, but, like other interferometric measurements, it requires good temporal coherence and involves considerable labor for its alignment. Researchers have also used spatially resolved spectral interferometry [5] and spatially resolved SPIDER [6,7], but these interferometric methods are also difficult to align and to keep aligned. SPIDER is also experimentally very complex and has within its apparatus a pulse stretcher, which significantly angularly disperses the beam and requires very careful alignment or it will itself introduce spatio-temporal distortions, including pulse-front tilt. In addition, spectral interferometry requires high stability of the absolute phase of the pulse to be measured. Adjustment of pulse-front tilt with a modified single-shot autocorrelator has also been suggested [8] and is available commercially as a "tilted-front-pulse autocorrelator". This device is often used in practice for revealing pulse-front tilt and adjusting the elements that cause it. However, it not only suffers from ambiguities in temporal intensity (and it does not measure the phase [9]), but also it only indicates the presence of pulse-front tilt qualitatively; it does not provide quantitative measurement of it or yield its sign.

In this note, we report a device for measuring pulse-front tilt that is simple, easy to use, reliable, artifact-free, and accurate. As in a previous publication [1], where we showed that GRENOUILLE [10] measures spatial chirp as well as the intensity and phase—*without a single modification*—here we show that GRENOUILLE also measures pulse-front tilt, and again it *also does so without a single modification*. Indeed, GRENOUILLE can measure both of these distortions both accurately and simultaneously—and in addition to the pulse intensity and phase.

This works because GRENOUILLE is a very symmetrical device, in which the pulses necessarily cross in space and time, typically at the center of the crystal, which can be made to coincide with the center of the CCD camera. Therefore, pulses without pulse-front tilt will generate their maximum-intensity second-harmonic signal at the center of the crystal (at zero relative delay). This also centers the trace on the camera. The effect of pulse-front tilt is then to move the traces off to one side or the other of the crystal. And the shift from the center of the crystal is proportional to pulse-front tilt angle. Since no other effect is known to cause such a shift, GRENOUILLE traces unambiguously reveal and measure pulse-front tilt and its relative, angular dispersion [2].

This means that GRENOUILLE, despite its ultrasimple apparatus, easily reveals a wide range of ultrashort-pulse characteristics: intensity and phase vs. time, spectrum and spectral phase, spatial chirp, and pulse-front tilt. And the apparatus can be easily bypassed, allowing the camera used for these measurements to easily reveal the beam spatial profile, too.

2. Theory of pulse-front tilt in GRENOUILLE measurements

We begin by showing that, although standard arrangements of single-shot SHG FROG measures spatial chirp, it does *not* measure pulse-front tilt. The usual expression for SHG FROG traces is similar to that for GRENOUILLE [11], so, to see the effect of pulse-front tilt on FROG traces, we start with the better known analytical expression for the SHG FROG trace:

$$I_{FROG}^{SHG}(\omega,\tau) = \left| \int_{-\infty}^{\infty} \{E(t)\exp[i\omega_0 t]\} \quad \{E(t-\tau)\exp[i\omega_0 (t-\tau)]\} \quad \exp[-i\omega t] \; dt \right|^2 \qquad (1)$$

In single-shot FROG, the effect of pulse-front tilt is to add a position-dependent time t(x) = ζx, where ζ is pulse-front tilt parameter, which can be expressed as ζ = δt/δx. Then the SHG FROG trace becomes:

#2097 - $15.00 US Received February 03, 2003; Revised March 01, 2003

$$I_{FROG}^{SHG\ pft}(\omega,\tau) \quad =$$

$$\left| \int_{-\infty}^{\infty} E(t+\zeta x)\exp[i\omega_0 t]\, E(t+\zeta x-\tau)\exp[i\omega_0(t-\tau)]\exp[-i\omega t]\, dt \right|^2 \tag{2}$$

where we have omitted the complex exponentials that will vanish when the magnitude is squared later. By changing variables, t' = t + ζx, we can simplify (2):

$$\left| \int_{-\infty}^{\infty} E(t')\exp[i\omega_0 t']\, E(t'-\tau)\exp[i\omega_0(t'-\zeta x-\tau)]\exp[-i\omega(t'-\zeta x)]\, dt' \right|^2 \tag{3}$$

$$= \left| \int_{-\infty}^{\infty} E(t')\exp[i\omega_0 t']\, E(t'-\tau)\exp[i\omega_0 t']\exp[-i\omega t']\, dt' \right|^2 \tag{4}$$

$$= I_{SHGFROG}(\omega,\tau) \tag{5}$$

This indicates that, for single-shot SHG FROG, pulses with tilted fronts yield the same expression as pulses without pulse-front tilt (Fig. 2), and hence the single-shot SHG FROG trace does not depend on, that is, does not measure, the pulse-front tilt.

However, GRENOUILLE is slightly different. Unlike SHG FROG, which usually uses a partial reflector to split the beam in two, GRENOUILLE splits the same pulse from the center (one side of the beam gates the other). As a result, *in GRENOUILLE, pulse-front tilt introduces an extra average delay, $+\tau_0$, in one pulse and an average advance $-\tau_0$ in the other*. Then the expression for GRENOUILLE traces, in the presence of pulse-front tilt becomes:

$$\left| \int_{-\infty}^{\infty} E(t+\tau_0+\zeta x)\exp[i\omega_0 t]\, E(t-\tau_0+\zeta x-\tau)\exp[i\omega_0(t-\tau)]\exp[-i\omega t]\, dt \right|^2 \tag{6}$$

Letting t' = t + τ_0 + ζx:

$$\left| \int_{-\infty}^{\infty} E(t')\exp[i\omega_0 t']\, E(t'-2\tau_0-\tau)\exp[i\omega_0(t'-\tau_0-\zeta x-\tau)]\exp[-i\omega(t'-\tau_0-\zeta x)]\, dt' \right|^2 \tag{7}$$

Canceling out the vanishing complex exponentials:

$$= \left| \int_{-\infty}^{\infty} E(t')\exp[i\omega_0 t']\, E(t'-2\tau_0-\tau)\exp[i\omega_0 t']\exp[-i\omega t']\, dt' \right|^2 \tag{8}$$

$$= I_{SHGFROG}(\omega,\tau+2\tau_0) \tag{9}$$

This last expression clearly indicates that pulses with tilted fronts yield GRENOUILLE traces that are shifted (on the delay axis), compared to pulses without pulse-front tilt (Fig. 3). It is possible to align the device so that the second-harmonic signal produced by pulses without pulse-front tilt is centered on the CCD camera. Therefore, any shift of the trace from the center can be attributed to pulse-front tilt, since no other effect causes such an asymmetry in GRENOUILLE traces.

Note also that this result is independent of the pulse intensity and phase; the method is general.

#2097 - $15.00 US Received February 03, 2003; Revised March 01, 2003

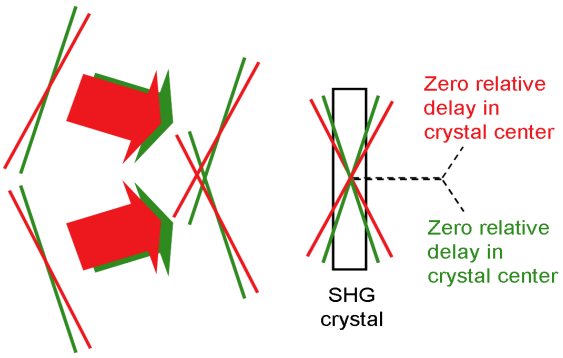

Fig. 2. Pulse-front tilt in single-shot SHG FROG: Pulses without pulse-front tilt (shown in green) yield traces centered on the crystal, where zero relative delay occurs. Pulses with pulse-front tilt (shown in red), also yield traces centered at the same point. Therefore, single-shot SHG FROG does not distinguish pulse-front tilt. (Magnitude of tilt exaggerated for clarity.) This is also true of other FROG beam geometries. Pulse-front tilt does, however, change the delay calibration, so this must be taken into account (using a reference double-pulse with known pulse separation as a calibration, as is commonly done).

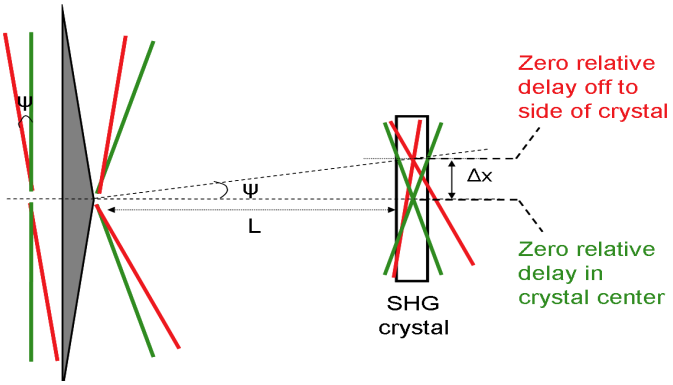

Fig. 3. Pulse-front tilt in GRENOUILLE: Pulses without pulse-front tilt (shown in green) yield traces centered at the crystal, where zero relative delay occurs. However pulses with pulse-front tilt (shown in red), cause the zero relative delay to be off to the side of the crystal, causing the trace to be shifted from the center of the crystal. The figure also shows calculation of pulse-front tilt from the amount of shift at the center of the trace. (Magnitude of tilt exaggerated for clarity.)

There is also a very small amount of pulse-front tilt imposed in each beam by the biprism, but it is of opposite sign for the two beams and does not introduce any trace displacement and hence does not bias the measurement. It does affect the delay calibration, but this is taken into account by the standard delay calibration methods and hence does not affect the measurement.

3. Numerical evaluation of the pulse-front tilt and extraction of the intensity and phase from a shifted trace

The shift of the trace from the center of the crystal reveals pulse-front tilt in the beam. It is also possible to extract the numerical value of pulse-front tilt from the amount of shift (Fig. 3). The tilt angle of the beam is can be written as [2, 12]:

#2097 - $15.00 US
Received February 03, 2003; Revised March 01, 2003

$$\tan\psi = c\frac{\partial t}{\partial x} = c\varsigma \tag{10}$$

From the figure, it is easy to note that another expression for this angle is:

$$\tan\psi = \frac{\Delta x}{L} \tag{11}$$

where L is the separation between Fresnel biprism and second harmonic crystal, and Δx is the shift of the trace center. Equating Eqs. (10) and (11) we obtain:

$$\zeta = \frac{\partial t}{\partial x} = \frac{\Delta x}{Lc} \tag{12}$$

This equation shows that the numerical value of pulse-front tilt is directly proportional to the amount of shift and the distance between the crystal and Fresnel biprism.

Finding the amount of shift and using Eq. (12) yields the pulse-front tilt, ζ. The shift can be found in several ways, but, for traces with Gaussian intensity profile, the peak of the trace can be found by a Gaussian fit at the central spectrum. Then the amount of shift is found simply by extracting the central delay from this value (note that, for GRENOUILLE, delay and position are proportional [11]). The pulse-front tilt can then be removed from the trace by simply translating to the center, which yields true GRENOUILLE trace for E(t):

$$I_{FROG}^{SHG}(\omega,\tau) = I_{FROG}^{SHG\ pft}(\omega,\tau - 2\tau_0) \tag{13}$$

The resulting trace is now the best estimate for the actual trace—and hence the pulse—in the absence of pulse-front tilt. The SHG FROG algorithm can then be run on the now symmetrical (centered) trace, yielding the pulse intensity and phase in the absence of pulse-front tilt. The pulse-front tilt can then be added back into the retrieved pulse, reproducing the pulse with the appropriate amount of pulse-front tilt. Note that a pulse with pulse-front tilt will typically be longer due to the concomitant angular dispersion and its spectral lateral walk-off [3]. The spectral lateral walk-off reduces the effective available bandwidth at a given point, thus increasing the pulse width.

The pulse can then be reconstructed using the retrieved intensity and phase and including the measured pulse-front tilt. Specifically, if the FROG algorithm returns an intensity, I(t), and phase, ϕ(t), then the pulse-front-tilted pulse field will be given by:

$$E(x,t) = \sqrt{I(t+\varsigma x)}\exp[i(t+\varsigma x)\omega_0 - i\phi(t+\varsigma x)]$$

where ζ is the measured pulse-front tilt.

4. Experiment

Probably the easiest way to introduce variable amounts of pulse-front tilt into an ultrashort pulse is to use a single prism (or grating) at different angles of incidence. We have performed one set of experiments using this method. However, this method only achieves large values of pulse-front tilt and in only one direction, so we have performed another set of experiments by using a "modified pulse compressor," which is a standard pulse compressor with one of the prisms placed on a rotation stage. As mentioned earlier, any amount of non-parallelism (or, in our case, deviation from the angle of minimum deviation) causes pulse-front tilt. Therefore, with this setup, we can deliberately misalign and align the pulse compressor to get zero, positive, or negative pulse-front tilt.

#2097 - $15.00 US Received February 03, 2003; Revised March 01, 2003

While there is little or no subtlety in our techniques for generating or measuring pulse-front tilt, there is a major subtlety in *understanding* it in real laser beams. For Gaussian beams, pulse-front tilt *changes as the pulse propagates (i.e., diverges or converges)* [3,13]. The change in the tilt depends on the beam parameters (spot size, the distance between the dispersive element and the beam waist, and the distance between the dispersive element and the observation point). And, depending on these parameters, this change can be very significant (Fig. 4). For all of the theoretical plots in this work, it was necessary to take into account the Gaussian behavior of the beam and its effects on the pulse-front tilt. For the sake of brevity, we omit our detailed calculations of the pulse-front tilt in our experiments, which included the change in pulse-front tilt with propagation, and which essentially mirrors that found in [13,14,15].

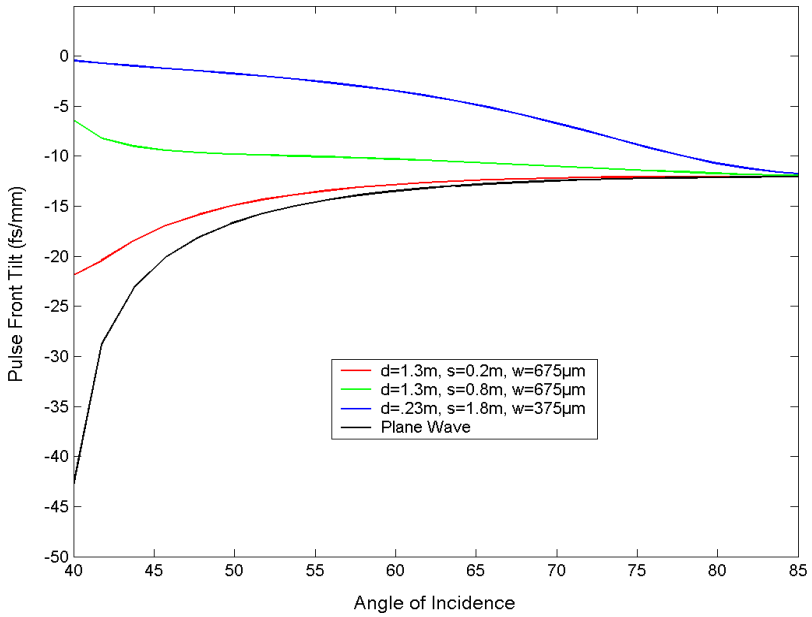

Fig. 4. Theoretical dependence of the pulse-front tilt on angle of incidence for plane waves (blue curve) and Gaussian beams with various beam parameters (other colored curves). A 69^0 apex-angle fused-silica prism is used for calculation. The parameters are; d, the distance between beam waist and prism; s, the distance between prism and observation point; w, the beam width. The variation in pulse-front tilt is due to a complex combination of diffraction and beam expansion due to refraction at the prism faces.

In our measurements, we used a GRENOUILLE device supplied by Swamp Optics, which incorporated a 168^0-apex-angle Fresnel biprism, various lenses, and 3-mm thick BBO crystal. The calibration was as follows; for a 256x240 array, delay axis was 7.12 fs/pix, and wavelength axis was 0.139 nm/pix.

Figure 5 shows measured GRENOUILLE traces for pulses with various amounts of pulse-front tilt, generated using our modified pulse-compressor. Note the significant variation of the displacement of the trace along the delay axis as the pulse-front tilt varies, as predicted by our theory. Note also the traces also possess shear, due to spatial chirp (part of spatial chirp is of course due to angular dispersion), but as we have shown in our previous note [1] and this one, effects of pulse-front tilt and spatial chirp on GRENOUILLE traces affect the GRENOUILLE trace in independent ways and so are easily both measured simultaneously. Therefore, existence of spatial chirp in the trace does not affect pulse-front tilt measurements.

Figure 6 shows a comparison of the measured pulse-front tilt using GRENOUILLE the theoretical pulse-front tilt for a pulse emerging from our modified pulse compressor, plotted

#2097 - $15.00 US Received February 03, 2003; Revised March 01, 2003

as a function of the prism angle of incidence. There is very good agreement between the two curves.

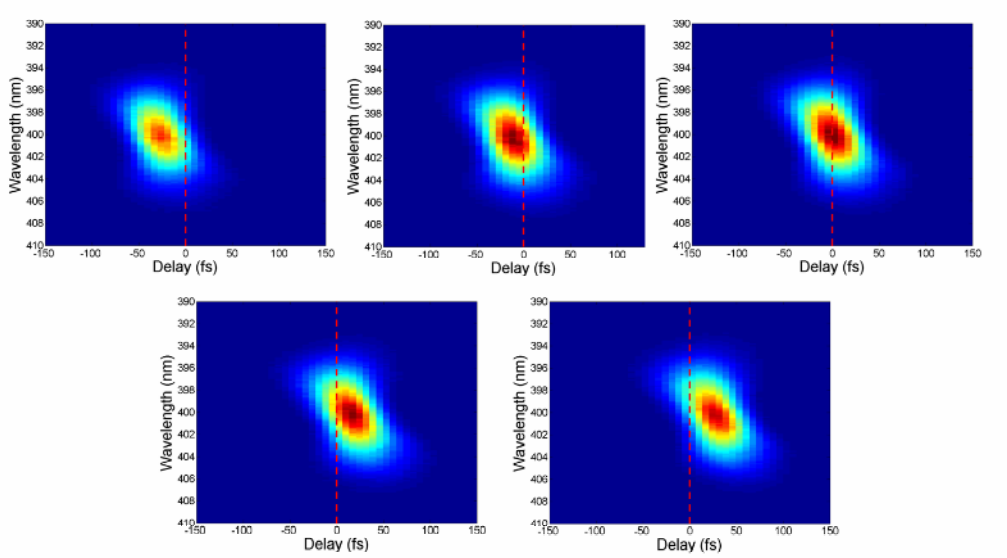

Fig. 5. Measured GRENOUILLE traces for pulses with very negative, slightly negative, zero, and slightly positive, and very positive pulse-front tilt. Notice that the trace displacement is proportional to the pulse-front tilt. The traces also possess some amount of shear, which indicates the existence of spatial chirp [1], but it has no effect on the center of the trace.

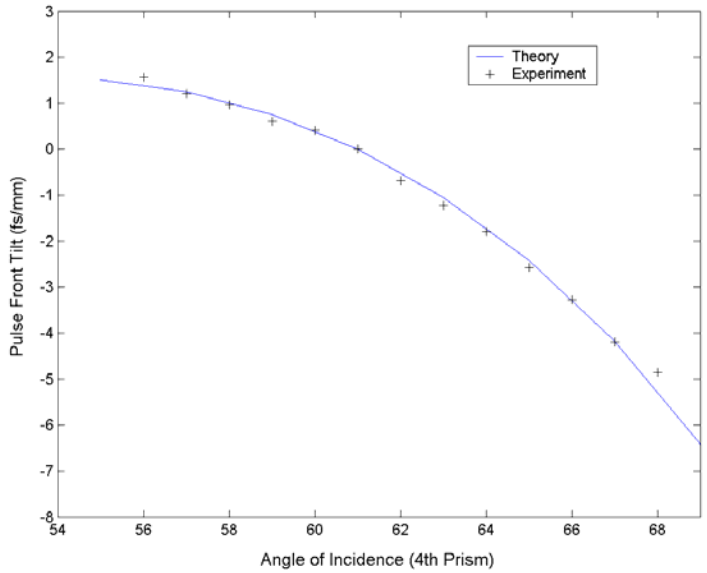

Fig. 6. Theoretically predicted pulse-front tilt and the experimentally measured pulse-front tilt using GRENOUILLE. The pulse-front tilt was varied using the modified pulse compressor described in the text. Note that, GRENOUILLE easily measures even small amounts of pulse-front tilt, such as occurs when the prism angle is at angle of minimum deviation, and zero pulse-front tilt is obtained, which corresponds to the case of the pulse-compressor being considered to be "aligned."

#2097 - $15.00 US
Received February 03, 2003; Revised March 01, 2003

Figure 7, on the other hand, shows an analogous plot that we obtained by using a single 69^0 apex angle, fused-silica prism. We again, have good agreement between the GRENOUILLE measurements and the theory.

GRENOUILLE can measure pulse-front tilt with high sensitivity. Using a Gaussian fitting to the intensity profile of the trace to find the center, we obtained a sensitivity in the measurement of pulse-front tilt of 0.05 fs/mm, which corresponds to a sensitivity in the measurement of angular dispersion of 0.12 μrad/nm. This sensitivity is even better than that reported using spectrally resolved interference (SRI) [4] (the sensitivity was reported to be 0.2 μrad/nm in that note). However, SRI, in principle, measures arbitrary orders of pulse-front tilt, whereas GRENOUILLE can measure only the first order.

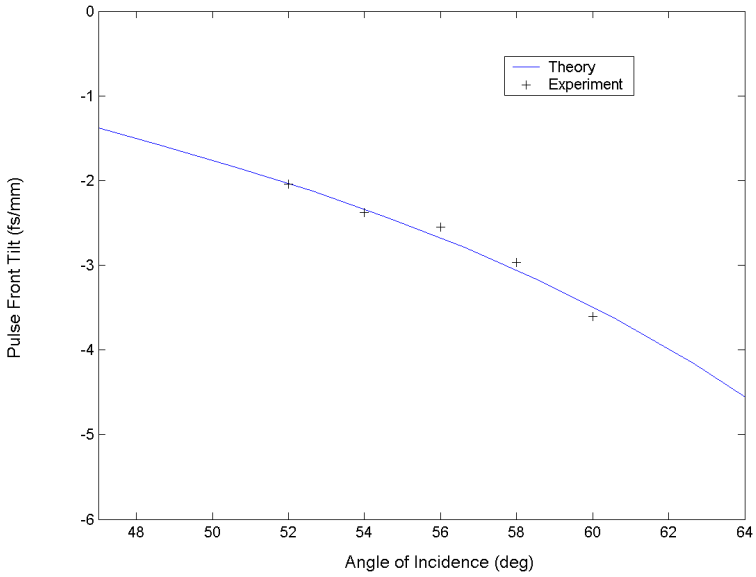

Fig. 7. Experimentally measured and theoretically predicted pulse-front tilt for our experiment performed by measuring pulses that have passed through a single fused silica prism. In this case the pulse front tilt is always negative (Theory curve is the blue curve in Fig. 4).

The fact that GRENOUILLE can measure pulse-front tilt with high sensitivity provides us the opportunity to align pulse compressors with a high sensitivity as well. We were able to align our prism pulse compressor with a sensitivity (in one prism angle of incidence) of 0.025 degrees. With such accuracy, this device should provide practical and reliable alignment of pulse compressors used in ultrafast laser laboratories.

6. Retrieval of Pulse in the Presence of Spatial Chirp

We also performed a preliminary test of our approach for determining the full spatio-temporal intensity and phase vs. time and position for a pulse with linear pulse-front tilt. Figure 8 shows the measured and retrieved GRENOUILLE traces for a pulse with no pulse-front tilt. Figure 9, on the other hand is the retrieval of the trace for pulse with pulse-front tilt (the amount of pulse front tilt for this pulse is 1.1 fs/mm). Notice the broadening of the pulse due to the narrower spectrum.

#2097 - $15.00 US Received February 03, 2003; Revised March 01, 2003

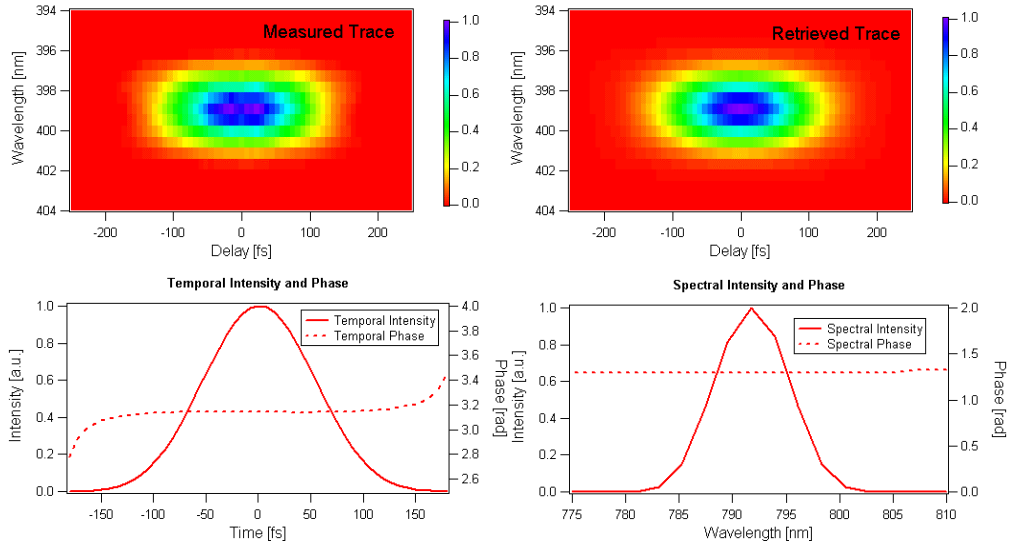

Fig. 8. Measurement of the intensity and phase of a pulse that does *not* have significant pulse-front tilt. The FWHM pulse width is 123.5 fs. The FROG error is 0.0039 (for a 128x128 array) for this measurement.

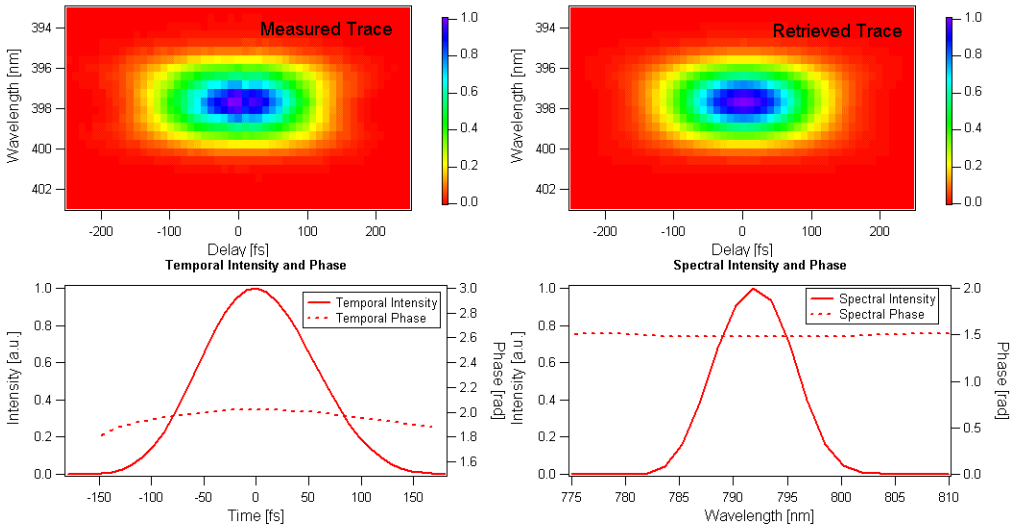

Fig. 9. Measurement of the intensity and phase of a pulse with pulse-front tilt. The FWHM pulse width is 125.1 fs. Note that the pulse broadens temporally due to spectral narrowing induced by spectral lateral walk-off. The FROG error is 0.0038 (for a 128x128 array) for this measurement.

7. Conclusion

In conclusion, we have demonstrated that the experimentally simple version of single-shot SHG FROG, GRENOUILLE, measures, not only the pulse temporal intensity and phase and spatial chirp, but also the pulse-front tilt. The trace shift from the center of symmetry is directly proportional to pulse-front tilt. The GRENOUILLE trace determines the full spatio-

#2097 - $15.00 US
Received February 03, 2003; Revised March 01, 2003

temporal characteristics of a pulse with pulse-front tilt. Finally, pulses frequently have simultaneous spatial-temporal distortions, spatial chirp and pulse-front tilt, and GRENOUILLE measures both of these distortions simultaneously.

Acknowledgements

This work was supported by National Science Foundation and a start-up grant from the Georgia Institute of Technology.

#2097 - $15.00 US Received February 03, 2003; Revised March 01, 2003